Korean J. Chem. Eng., 37(2), 216-223 (2020)
DOI: 10.1007/s11814-019-0445-1

pISSN: 0256-1115
eISSN: 1975-7220

Synthesis of Co-doped micro-mesoporous SAPO-11 zeolite for glycerol hydrogenolysis

Xue Li and Dongfang Wu†

Department of Chemical Engineering, School of Chemistry and Chemical Engineering,
Southeast University, Jiangning District, Nanjing 211189, China
(*Received 22 July 2019 • accepted 1 December 2019*)

Abstract−Co-doped micro-mesoporous SAPO-11 zeolite (Co-MSAPO-11) was synthesized and used for hydrogenolysis of glycerol. After simultaneous introduction of Co and mesopores, the pore structure and acidic properties of microporous SAPO-11 zeolite are reintegrated. The larger mesopores of Co-MSAPO-11 facilitate the diffusion of molecules and provide more space for the highly dispersed Co species. The appropriate acidity of Co-MSAPO-11 with more Lewis acid sites appears to be more helpful for the activation of reactants to intermediates, potentially increasing the probability of high selectivity to 1,2-propanediol. Therefore, Co-MSAPO-11 shows unique catalytic performance with a glycerol conversion of 94.0% and selectivity to 1,2-PDO of 90.5% under mild conditions. The possible representative model of Co-MSAPO-11 is proposed for the first time.

Keywords: Co, Acid Sites, Mesopores, SAPO-11, Glycerol Hydrogenolysis

INTRODUCTION

Glycerol is a cheap and readily available renewable resource [1]. With the depletion of non-renewable resources and the deteriorating environment, the utilization of glycerol to catalyze hydrogenolysis to form propanediol (PDO) will increasingly show its strong development potential and continue to be one of the hotspots of research and development worldwide [2-4]. Glycerol has one more hydroxyl group than PDO, the process of glycerol to PDO involves removing one hydroxyl group and adding one hydrogen atom. This is the same as removing a water molecule and adding a hydrogen molecule. In an acidic atmosphere [5,6], hydrogenolysis of glycerol to PDO has the following two steps on acid-metal bifunctional catalyst: a) glycerol is first dehydrated to form intermediate at acid sites; and b) the intermediate is further hydrogenated to produce PDO at metal sites. When the hydroxyl group in the terminal carbon of glycerol is attacked by a proton, the product is acetol and then 1,2-PDO is generated. In other cases, when the hydroxyl group in the middle of glycerol is attacked by protons, 3-hydroxypropanal can be produced and subsequently 1,3-PDO is produced. However, many reports have shown that it is easier to form 1,2-PDO instead of 1,3-PDO, probably because the intermediate acetol is more stable than 3-hydroxypropionaldehyde [7]. 1,2-PDO is an indispensable raw material for polyesters resins and widely used in the food, pharmaceutical and cosmetic industries [5]. Therefore, selective hydrogenolysis of glycerol to produce 1,2-PDO is of particular importance.

In recent years, various acid-catalyzed supports including SiO_2 [8-11], ZrO_2 [12,13], SBA-15 [14,15], TiO_2 [5,16], Amberlyst 15 [17] and the like have been applied for glycerol conversion. Among them, because of the moderate acidity and shape selectivity, microporous/mesoporous zeolite has received much attention and become one of the research goals in the field of material synthesis. It solves the problem of difficulty in separation and recovery of heterogeneous catalyst and avoids corrosion of equipment by strong acid catalyst. Suprun et al. [18] tested the catalytic performance of SAPO-11 zeolite for the dehydration of glycerol and showed high conversion of glycerol but low selectivity to the dehydrated product acetol. It has been recognized that SAPO-11 as a microporous zeolite with small pore size is not conducive to the adsorption and diffusion of macromolecules, which seriously suppresses macromolecules to active centers [19-21]. In our previous work [22], we demonstrated that micro-mesoporous SAPO-11 zeolite could be an effective acid support for hydrogenolysis of glycerol to commercial 1,2-PDO. Therefore, we hope to further synthesize micro-mesoporous SAPO-11 zeolite with larger mesopore diameters and special acidic properties to promote the efficiency of glycerol conversion.

Generally, precious metal (Pt, Ru, Ir) [23-27] and non-precious metal (Cu, Ni, Co) [28-33] catalysts have been examined for the hydrogenolysis of glycerol. Among the inexpensive, resource-rich non-precious metals, a number of related researches on Co catalysts have been reported, which has led to widespread interest in Co catalysts. Raksaphort et al. [32] reported that Co/γ-Al_2O_3 exhibited the highest glycerol conversion of 70.5% in all supported Co catalysts when the reaction conditions were 2.0 MPa initial H_2 pressure, 200 °C and 6 h. A MgO-supported Co catalyst used for glycerol hydrogenation possessed low catalytic activity with the conversion of glycerol at about 44.8% and target product 1,2-PDO selectivity of 44.2% because large by-products were obtained at short reaction time [33]. However, the catalytic performance of Co catalysts is not particularly good and most of them are common supported Co catalysts. However, a few studies have investigated the catalytic application of Co catalyst without loading of any Co

†To whom correspondence should be addressed.
E-mail: dfwu@seu.edu.cn

metal which was prepared by mixing Co precursor with support gel for hydrogenolysis of glycerol. Compared to supported catalysts, Co doped catalyst skips metal incipient wetness and secondary calcination process to reduce catalyst loss and could be used as bifunctional catalyst directly after being reduced. Therefore, it is a facile and attractive strategy to synthesize Co metal doped catalyst for this reaction.

Combined with the above, we first prepared micro-mesoporous SAPO-11 and their derivatives with Co doping into the SAPO-11 skeleton by mixing Co precursor with zeolite synthesis gel and then applied it to hydrogenolysis of glycerol to form 1,2-PDO. Further, for comparison, micro-mesoporous SAPO-11 zeolite supported Co catalysts were synthesized by incipient wetness technique. The effects of Co metal content and various reaction conditions on hydrogenolysis of glycerol were discussed.

EXPERIMENTAL

1. Materials

Pseudo-boehmite (72 wt% Al_2O_3) was supplied by Zibo Baida Chem. ind. Co., Ltd. DM-3010 (AR, 99 wt%) was obtained from Adamas Reagent, Ltd. Silica sol (30 wt%) was purchased from Qingdao Haiyang Chem. Co., Ltd. $Co(NO)_2{\cdot}6H_2O$ (99%), phosphoric acid (H_3PO_4, AR, 85 wt%), di-n-propylamine (DPA, AR, 98%), glycerol (ACS, 99.5%), 1,2-propanediol (1,2-PDO, AR, 99%) and 1-propanol (1-PO, AR, 99%) were obtained from Macklin Biochemical Co., Ltd. Acetol (AR, 99%), ethylene glycol (EG, AR, 99%) ethanol (AR, 99%) and methanol (AR, 99%) were supplied by Sinopharm Chemical Reagent Co., Ltd. (Beijing, China). All reagents were used as received.

2. Catalyst Preparation

There was simultaneous introduction of Co and mesopores into SAPO-11 zeolite (Co-MSAPO-11) with the final molar ratio of $Al_2O_3/P_2O_5/0.3SiO_2/1.2DPA/x Co/0.5059DM\text{-}3010/40H_2O$, where x stands for the Co doped content. The samples were named as MSAPO-11, 1Co-MSAPO-11, 3Co-MSAPO-11, 5Co-MSAPO-11 (abbreviated as Co-MSAPO-11 for sequence discussion) and 7Co-MSAPO-11 when x=0, 1, 3, 5 and 7, indicating that the doped amount of Co is 0, 1, 3, 5 and 7 wt%, respectively. MSAPO-11 also represents micro-mesoporous SAPO-11 zeolite. The small amine DPA as a microporous template. DM-3010 (N,N-dimethyl-N-octadecyl-N-(3-triethoxysilylpropyl) ammonium bromide) as mesoscale template belongs to a new class of cationic surfactants. In a common experimental process [1,2], a specific amount of cobalt nitrate was added to the gel with the initial composition of $Al_2O_3/P_2O_5/0.3SiO_2/1.2DPA/40\ H_2O$. Subsequently, a certain amount of DM-3010 was added to the previous gel. After 4 h of vigorous stirring, the mixture was statically crystallized in a 200 °C reactor for 12 h to synthesize Co-MSAPO-11. Meanwhile, ordinary microporous SAPO-11 zeolite (SAPO-11) was obtained without the addition of DM-3010 and Co source during the synthesis process. Co-SAPO-11 with Co theoretical content of 5 wt% was prepared with the DM-3010 not added. The Co catalyst supported on MSAPO-11 (Co/MSAPO-11) was synthesized by the impregnation method. The loaded Co content of Co/MSAPO-11 was 5 wt%. After drying at 120 °C for 12 h and subsequent calcination at 600 °C for 6 h, catalyst precursors were obtained. Finally, the above calcined sample was sieved into 100 mesh before use.

3. Characterization

X-ray diffraction (XRD) profiles of the calcined samples were obtained using a D/max-A diffractometer with Cu Kα radiation (λ=0.1542 nm). Diffraction lines of 2θ between 5° and 60°. N_2 adsorption-desorption isotherms were observed from a Micromeritics ASAP 2020 M apparatus. The specific surface area was calculated by the BET method, while the pore size distribution was evaluated by the BJH model. NH_3-TPD was analyzed by a Micromeritics ASAP2920 apparatus. A 0.2 g powder sample was initially purged in helium stream for 60 min at 450 °C and then decreased to 100 °C. NH_3 adsorption was carried out in a stream of NH_3-He (5 vol% NH_3) for 30 min at 50 cm^3/min and then blown in helium flow at 100 °C for 60 min. The signal peak of the desorbed NH_3 was recorded from 100 to 650 °C with a heating rate of 15 °C/min. The catalyst total acidity was evaluated by the peak area under ammonia desorption curve. The pyridine-adsorbed IR (Py-IR) on catalysts were carried out on a Thermo Fisher Nicolet 6700 spectrometer. A self-supporting wafer of the catalyst was initially dehydrated at 400 °C for 60 min under a vacuum atmosphere and then exposed to pyridine vapor for 30 min at 30 °C. Finally, after the evacuation of the system at different temperatures, the corresponding IR spectrum was recorded. The actual Co content was performed on inductively coupled plasma optical emission spectrometry (ICP-OES) with a PerkinElmer 3300DV emission spectrometer. Prior to testing, samples were reduced for 4 h at 600 °C under a stream of H_2.

4. Catalyst Assessment

Before testing, the powder sample was reduced in a 120 mL/min H_2 flow at 600 °C for 4 h and then cooled to ambient temperature in H_2 flow. Hydrogenolysis of glycerol was examined in a high pressure reactor (250 mL). First, 5.0 g glycerol was diluted by 60.0 g deionized water. 1.0 g catalyst was mixed with the above solution in the autoclave. After the reaction device was assembled, it was subjected to the following operations such as leak detection and air discharge. Finally, the reactor was set at the desired initial H_2 pressure (2.0-5.0 MPa) and temperature (200-230 °C). The reaction time started from the temperature reaching the set value. Consequently, the obtained reaction solution was first naturally cooled and then analyzed by a gas chromatograph (GC-126) equipped with FID (It is prepared for all the tested chemicals, including glycerol, 1,2-PDO, 1-PO, EG, acetol, ethanol, and so on.) connected to an SE-54 capillary column (30 m×0.32 mm×0.25 μm). The carbon loss was always less than 2% and almost 100% of carbon balance was achieved. The conversion of glycerol and each product selectivity were calculated by the following equations:

$$\text{Glycerol conversion (\%)} = \frac{\text{moles of glycerol converted}}{\text{moles of initial glycerol}} \times 100 \quad (1)$$

$$\text{Product selectivity (\%)} = \frac{\text{C-based moles of specific product}}{\text{sum of C-based moles of all products}} \times 100 \quad (2)$$

5. Circular Test

Circular tests in glycerol hydrogenolysis were conducted over Co-MSAPO-11 catalyst when the reaction conditions were 220 °C, 4.0 MPa initial H_2 pressure and 8 h. At the end of each cycle reac-

tion, the system was centrifuged, followed by filtrating. The reaction solution in the flask was analyzed by gas chromatograph. The residual catalyst was dried in the oven at 120 °C overnight, and then calcined at 450 °C for 4 h to remove deposited carbon. The pre-reduced catalyst was again used to test the catalytic reaction.

RESULTS AND DISCUSSION

1. Catalyst Characteristics

The XRD patterns of the synthesized samples are depicted in Fig. 1. For each sample, the main crystallites of SAPO-11 (JCPDS PDF No. 00-047-0614) are observed and no other impure phase is generated, which suggests all the samples were successfully prepared [21]. Regarding Co catalysts, a peak associated with Co was not observed. It is speculated that Co species probably are well dispersed. Moreover, the actual Co content of the Co/MSAPO-11 and Co-MSAPO-11 catalysts was directly detected by ICP characterization, as shown in Table 1. The actual Co content of Co-MSAPO-11 is closer to the theoretical value of 5 wt% than that of Co/MSAPO-11. It can be seen that the Co species are more likely to enter into the skeleton of the MSAPO-11 zeolite in a directly doped manner, rather than in a supported manner. The strong interaction between Co metals and MSAPO-11 in Co-MSAPO-11 catalyst results in the presence of more Co metals. Besides, the larger pore size of Co-MSAPO-11 could accommodate more Co metals and allow them to disperse better. The pore size data for the Co-MSAPO-11 and Co/MSAPO-11 samples are given in the subsequent N_2-physical adsorption experiments.

As illustrated by the N_2-physisorption isotherms in Fig. 2(a), except for SAPO-11 zeolite, all other samples are type IV isotherms with an H_4 hysteresis loop in the range of relative pressure from 0.45 to 0.95, indicating the presence of mesopores [21]. Table 1

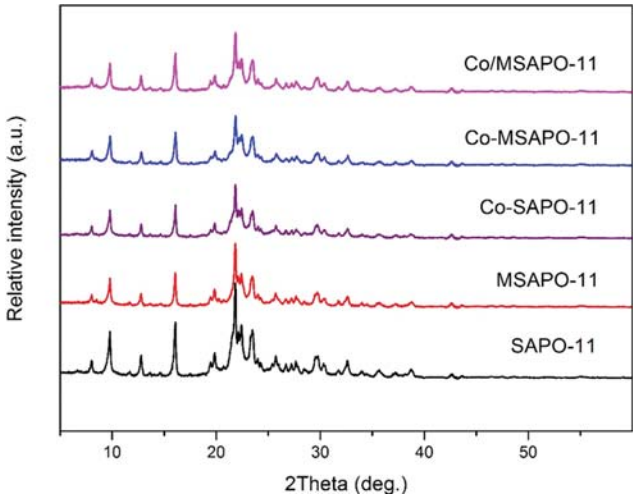

Fig. 1. XRD patterns of the catalyst samples.

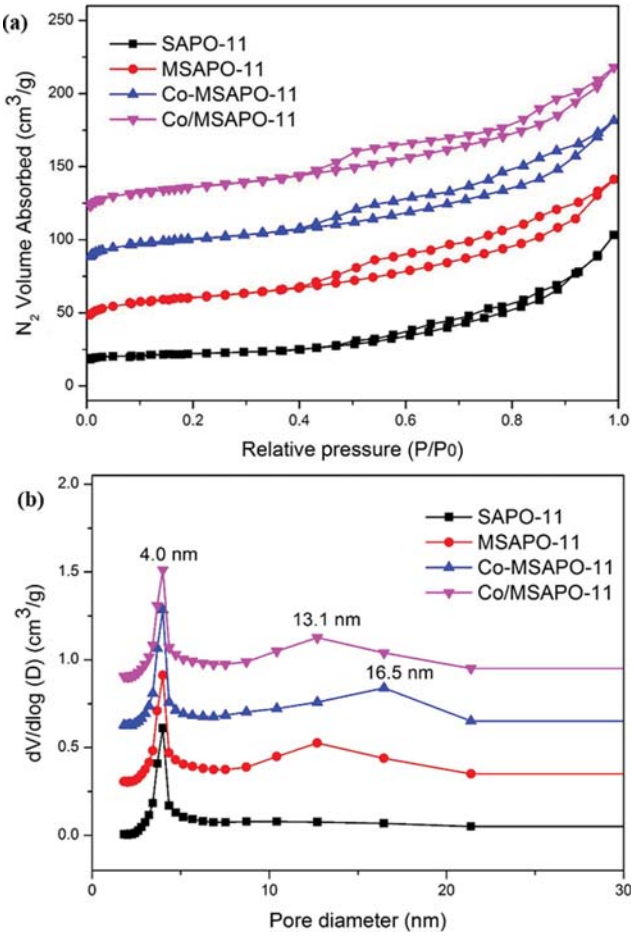

Fig. 2. (a) Nitrogen adsorption-desorption isotherms and (b) pore size distributions of the catalyst samples. The isotherms of MSAPO-11, Co-MSAPO-11 and Co/MSAPO-11 samples have been offset by 40, 80 and 120 cm^3/g along the vertical axis for clarity, respectively. Their pore size distributions have also been offset by 0.3, 0.6 and 0.9 cm^3/g, respectively.

Table 1. Physicochemical properties of the prepared samples

Sample	S_{BET} $[m^2/g]^a$	S_{ext} $[m^2/g]^b$	V_{meso} $[cm^3/g]^c$	V_{micro} $[cm^3/g]^d$	Acidity [μmol/g]	Co content [wt%]
SAPO-11	185	91	0.08	0.05	368.4	--
M-SAPO-11	319	165	0.28	0.04	435.7	--
Co-MSAPO-11	237	124	0.20	0.02	306.3	4.5
Co/MSAPO-11	252	108	0.16	0.02	267.3	4.1

[a]BET surface area.
[b]External surface area, obtained from *t*-plot method.
[c]Mesoporous pore volume, obtained from BJH method.
[d]Microporous pore volume, obtained from *t*-plot method.

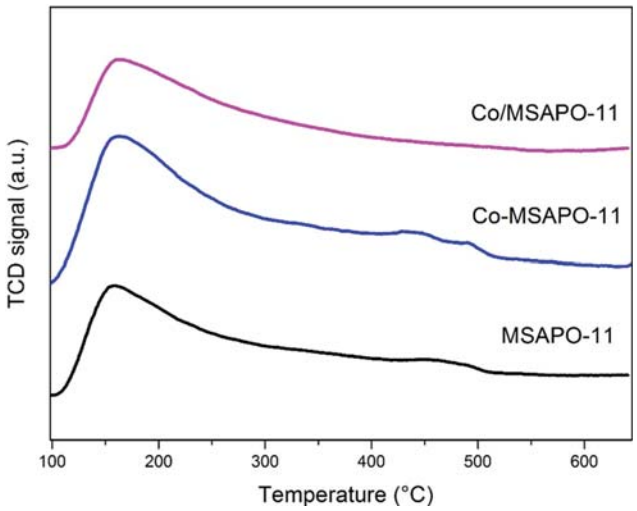

Fig. 3. NH_3-TPD profiles of the MSAPO-11, Co-MSAPO-11 and Co/MSAPO-11 samples.

summarizes the textural properties of the samples. MSAPO-11 exhibits the highest surface area of 319 m^2/g and pore volume of 0.32 cm^3/g. After loading Co, both the surface area and total pore volume of Co/MSAPO-11 decrease. The decrease in the BET surface area of Co/MSAPO-11 may be attributed to secondary calcination after loading Co. The metals might block the channel of the catalyst and make the total pore volume drop. Similarly, Co-MSAPO-11's total pore volume and mesopore volume are reduced. The pore size distribution curves (Fig. 2(b)) are consistent with the results of the above N_2-physisorption curve. The pore size distributions of MSAPO-11 and Co/MSAPO-11 are very similar and stable at 4 and 13.1 nm. The main pore size distribution of Co-MSAPO-11 is at 16.5 nm, which is higher than that of Co/MSAPO-11. This may be because the doped Co atoms enter the zeolite framework, thereby changing the pore structure of the zeolite.

An NH_3-TPD experiment was conducted to study the acidic properties of MSAPO-11, Co/MSAPO-11 and Co-MSAPO-11. Fig. 3 shows the NH_3-TPD curves of all samples. The main desorption peak at about 200 °C is assigned to weak acid sites, while the weak desorption peak at about 450 °C is due to the stronger acid sites [34]. Thus, SAPO-11 is a characteristic medium-strong acid zeolite, which is consistent with earlier literature [35]. Both Co/MSAPO-11and Co-MSAPO-11 have stronger acidity than MSAPO-11 because their main desorption peaks are shifted to higher temperature. As listed in Table 1, the total acidity of Co catalysts is decreased compared to MSAPO-11. However, the Co-MSAPO-11 catalyst has higher total acidity than that of Co/MSAPO-11. The possible reason is that Co might be doped into MSAPO-11 skeleton in Co-MSAPO-11 catalyst, resulting in less Co metal species occupying acid site centers. Additionally, the larger mesoporosity of Co-MSAPO-11 than Co/MSAPO-11(Fig. 2(b)) might let more acid sites be exposed.

The Py-IR spectrum of Co-MSAPO-11 catalyst at different temperatures is shown in Fig. 4(a). The band at approximately 1,445 cm^{-1} can be attributed to the chemisorption of pyridine on Lewis (L) acid sites. Correspondingly, the band at about 1,540 cm^{-1} indicates some Brönsted (B) acid sites are distributed in the internal and/or surface of Co-MSAPO-11 [19]. With regard to the band at about 1,490 cm^{-1} detected, which is usually attributed to the 19a mode vibration of pyridine associated both Brönsted and Lewis acid sites and a contribution about 1,600 cm^{-1} could be due to two bands generated by acid sites with different nature. It is found that all band's intensity and area are reduced as the desorption temperature increases, which indicates Co-MSAPO-11 has less strong acid sites. Because, the band at high temperature (for example, 350 °C) corresponds to strong acid sites of catalyst. As shown in Fig. 4(b), to figure out the differences of acidic properties between Co/MSAPO-11 and Co-MSAPO-11 catalysts, their Py-IR spectra at 150 °C are compared. The peak intensity of Co/MSAPO-11 is lower than that of Co-MSAPO-11. This roughly estimates that Co-MSAPO-11 has a greater number of L acid sites and B acid sites than Co/MSAPO-11. Since glycerol is dehydrated to form intermediate acetol occurring at the acid sites, so in addition to metal species, acidity is one of the essential factors in the catalytic performance of catalyst. Relevant literature [36] reports that L acid sites appear to be more prone to interact with the terminal hydroxyl

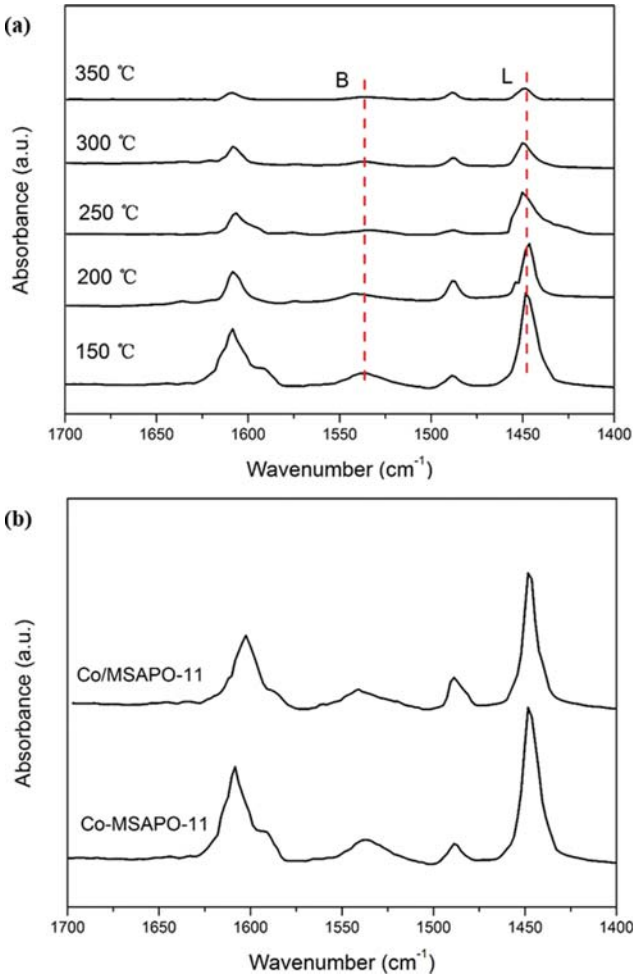

Fig. 4. (a) Pyridine-IR spectra of Co-MSAPO-11 at different temperature and (b) Pyridine-IR spectra of Co-MSAPO-11 and Co/MSAPO-11 at 150 °C.

Table 2. Lewis acidity of Co/MSAPO-11 and Co-MSAPO-11

T [°C]	L acid [μmol/g]	
	Co/MSAPO-11	Co-MSAPO-11
150	130	183
200	59	76
250	36	53
300	16	24
350	10	15

groups of glycerol, thereby dehydrating glycerol to the intermediate acetol, and then acetol produces the target product, 1,2-PDO, at the metal sites. Therefore, samples with more L acid sites may be effective catalysts for the hydrogenolysis of glycerol. As shown in Table 2, at a minimum temperature of 150 °C, the L acidity of Co-MSAPO-11 is 185 μmol/g, while the L acidity of Co/MSAPO-11 is 130 μmol/g. As the temperature increases, the amount of L acid in both samples gradually decreases, but the amount of L acid in Co-MSAPO-11 is always higher than that in Co-MSAPO-11. Thus, the Co-MSAPO-11 catalyst may have better activity in hydrogenolysis of glycerol.

2. Possible Model of Co-MSAPO-11

The possible representative skeleton structure of Co-MSAPO-11 is shown in Fig. 5. It is well known the formation of SAPO-11 by the Si atom introduced into the neutral AlPO-11 skeleton. It involves two kinds of substitution mechanisms [37]: a) as shown in the lower right corner of Fig. 5, a P atom is substituted by a Si atom; b) as shown in the upper left corner of Fig. 5, an adjacent Al atom and P atom are simultaneously substituted by two Si atoms.

In addition, the missing portion is assumed to represent a possible mesoporous structure in the microporous SAPO-11 zeolite. It is created by mesoscale template DM-3010. Because the surface of the zeolite is negatively charged, DM-3010 molecules can be attached to the zeolite precursor by chemical bonds. Their long-chain alkylammonium moieties can be removed during sample calcination. In this way, some space is left and the mesopores are obtained. The mesopores accelerate the mass transfer of macromolecules and achieve high Co dispersion.

The metal Co in Co-MSAPO-11 catalyst is capable of providing a hydrogenation active site in the hydrogenolysis of glycerol, so

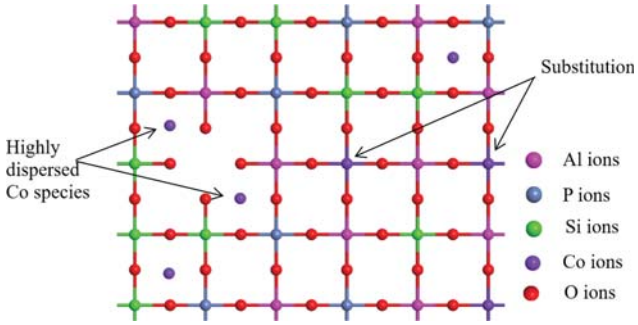

Fig. 5. The possible model of Co-MSAPO-11.

it is necessary to determine the position at which Co is located. Co-related species may exist in three forms (Fig. 5): a) a portion of Co may be dispersed in the mesopores in MSAPO-11; b) some Co metal species could have a strong interaction with SAPO-11, some of which are highly likely to be doped into zeolite lattices [38,39], so that a kind of Co atom substitution might change zeolite's Al or P atoms arrangement; and c) Co species may be present in the pores of catalyst in an aggregated manner, not shown here.

3. Comparison of Different Catalysts

The hydrogenolysis of glycerol uses a classical batch reactor with a heterogeneous catalyst based on MSAPO-11 zeolite, modified by Co doping. The liquid products of glycerol conversion include 1,2-PDO, 1-PO, EG, acetol, and a small amount of ethanol. Since Co species in catalyst is an important factor affecting the conversion of glycerol, the reaction was performed over *x*Co-MSAPO-11 catalysts, and the experimental data is displayed in Table 3 (entry 1 to 4). As the amount of Co doping increases from 1 to 7 wt%, the conversion of glycerol increases sharply from 35.1% (*x*=1 wt%) to the maximum value at about 67.1% (*x*=5 wt%), and then shows a decrease to 61.9% (*x*=7 wt%). It is apparent that appropriate Co metal doping amount can efficiently speed up the reaction; however, excessive Co doping amount might occupy large active sites, resulting in lower glycerol conversion. The 1,2-PDO selectivity increases steadily to about 94.8%, which is remarkably related to the range of Co amount. Because of the presence of more Co metal sites, the hydrogenation of intermediates acetol could quickly increase to form 1,2-PDO.

To further evaluate the catalytic performance of 5Co-MSAPO-

Table 3. Glycerol Conversion over different catalysts[a]

Entry	Catalyst	Conversion [%]	Selectivity [%]			
			1.2-PDO	1-PO	EG	Others
1	1Co-MSAPO-11	35.1	60.7	2.2	9.3	27.8
2	3Co-MSAPO-11	58.0	81.0	3.4	3.3	12.5
3	5Co-MSAPO-11	67.1	94.8	4.0	1.2	0.2
4	7Co-MSAPO-11	61.9	95.0	3.8	0.0	1.2
5	Co-SAPO-11	52.1	72.5	8.8	7.3	11.4
6	Co/MSAPO-11	57.9	86.0	2.0	5.7	6.3
7	MSAPO-11	32.7	0.0	0.0	0.0	100
8	SAPO-11	19.3	0.0	0.0	0.0	100

[a]Reaction conditions: 4.0 MPa H_2, 210 °C, and 8 h.

11 (consistent with the above, abbreviated as Co-MSAPO-11), Co-SAPO-11 and Co/MSAPO-11 catalysts were used as a comparison for glycerol hydrogenation to 1,2-PDO. As illustrated in Table 3 (entries 3, 5 and 6), the conversion of glycerol and product selectivity are greatly affected by the type of catalysts. Co-SAPO-11 shows the low catalytic performance for glycerol hydrogenation with the conversion of glycerol is only 52.1%, and the 1,2-PDO selectivity of 72.5% (entry 5). It is shown that the small pore size in Co-SAPO-11 limits the mass transfer of glycerol and/or products, with the result that the overall hydrogenated reaction is inhibited. However, Co-MSAPO-11 catalyst possesses superior catalytic activity than does Co-SAPO-11. Based on the related NH_3-TPD and N_2-physical adsorption characterizations, there are three possible explanations. First, more acid sites of Co-MSAPO-11 is beneficial to the dehydration of glycerol to intermediates, providing more possibilities for further generation of target products 1,2-PDO. Second, the large generated mesopores in Co-MSAPO-11 increase the connectivity of the framework and greatly reduce the diffusion limitation of the reagents, thereby hindering the consecutive reactions. Finally, the large mesopores might make Co species better dispersed. The well dispersed Co species could contribute greatly to the hydrogenation of intermediates to 1,2-PDO.

A conventional supported catalyst, Co/MSAPO-11, was prepared by impregnation method for glycerol conversion and its catalytic activity results are also illustrated (entry 6). The conversion of glycerol (57.9%) and the 1,2-PDO selectivity (86.0%) are attained. However, they are all lower than that of the doped Co-MSAPO-11 catalyst (entry 3). There is a close correlation between catalyst properties (acidity, redox properties) and catalytic performance. NH_3-TPD results suggest that Co-MSAPO-11 has more total acidity than Co/MSAPO-11 (Table 1), which favors the conversion of glycerol to intermediates acetol. Py-IR characterization allows us to further explore the effect of acidity on the reaction. As expected, more L acid sites in Co-MSAPO-11 have a very positive effect on the conversion of glycerol to intermediates. As ICP characterization and N_2-physical adsorption confirmed, Co-MSAPO-11 has more actual Co content and larger mesopores than Co/MSAPO-11 (Table 1), which could facilitate the conversion of glycerol to desired products obviously. It is also pointed out that the different methods of preparing Co catalysts affect the chemical environment of Co metals. More specifically, Co species might easily enter into the MSAPO-11 skeleton in a directly doped manner [38], which decreases the loss of active metal sites. The strong interaction between Co and MSAPO-11 could prevent Co metals escaping from the catalyst during the liquid phase reaction. As mentioned, the hydrogenolysis of glycerol is greatly accelerated over Co-MSAPO-11 because of the better metal-acid synergistic effect.

Furthermore, by comparison with SAPO-11 and MSAPO-11 (entries 7 and 8), Co-MSAPO-11 also shows higher catalytic activities. It can be seen that the order of glycerol conversion, Co-MSAPO-11>MSAPO-11>SAPO-11, aligns with their pore diameters sequence. This demonstrates the advantage of more mesopores. Notably, when employing SAPO-11 and MSAPO-11 as catalysts, there are large numbers of byproducts (e.g., intermediate acetol) in the liquid phase. Since SAPO-11 and MSAPO-11 are only acidic, glycerol can only form dehydration products at acid active sites. However, the incorporation of Co in Co-MSAPO-11 catalyst has a strong disposition to form target product 1,2-PDO that is generated from intermediate hydrogenation at metal active sites. All results prove that the presence of mesopores and Co metal increases glycerol conversion growth and then is favorable for 1,2-PDO formation.

4. Effects of Reaction Conditions

Whether catalyst can be applied to industry often depends on the required different reaction conditions of a catalytic reaction. Therefore, the effects of different reaction time, temperature and initial H_2 pressure on glycerol conversion over Co-MSAPO-11 catalyst need to be investigated. As clearly indicated in Table 4 (entry 1 to 3), when the examined reaction time rises from 4 h to 8 h, the conversion of glycerol and the target product selectivity are continuously increased, but the rate of 1,2-PDO selectivity increases slowly. As the reaction time is 10 h (entry 4), the reaction mostly reaches thermodynamic equilibrium. If the reaction time is continuously prolonged, it may lead to the formation of many by-products. Taking into account the above factors, 8 h is determined as the optimal reaction time.

Table 4. Hydrogenolysis of glycerol over Co-MSAPO-11 under different conditions

Entry	t [h]	P [MPa]	T [°C]	Cov. [%]	Selectivity [%]			
					1.2-PDO	1-PO	EG	Others
1	4	4	210	42.2	80.9	10.1	6.2	3.8
2	6	4	210	60.8	92.0	4.6	2.3	1.0
3	8	4	210	67.1	94.6	4.0	1.2	0.2
4	10	4	210	69.6	93.2	3.3	3.5	0.0
5	8	4	200	27.0	83.5	11.1	0.5	4.9
6	8	4	210	67.1	94.6	4.0	1.2	0.2
7	8	4	220	90.9	87.6	3.5	8.3	0.6
8	8	4	230	95.3	80.0	3.2	13.5	3.3
9	8	2	220	58.4	75.3	7.0	14.2	3.5
10	8	3	220	70.4	82.0	3.7	10.1	4.2
11	8	4	220	90.9	87.6	3.5	8.3	0.6
12	8	5	220	94.0	90.5	2.0	8.5	0.0

As depicted in Table 4 (entry 5 to 8), the experiments of glycerol conversion proceeded over Co-MSAPO-11 catalyst at different reaction temperature from 200 to 230 °C. Note that during reactor heating, the chamber pressure continues to increase, but decreases as the reaction proceeds. When the reaction temperature rises in the range from 200 to 230 °C, glycerol conversion significantly enhances from 27.0% to 95.3%. As expected, high temperature activates more reactive molecules and increases the chance of molecular collisions to improve the conversion of glycerol. The selectivity of 1,2-PDO first improves from 83.5% to the maximal value (94.6%) at 210 °C and then decreases obviously. It is consistent with the previous work of Gong et al. They reported that the increase in reaction temperature greatly promotes the formation of intermediates acetol by glycerol dehydration, making glycerol more prone to convert to 1,2-PDO [40]. Nevertheless, the higher reaction temperature results in a decrease in 1,2-PDO selectivity. This can be interpreted by that a large amount of cracking products EG are formed at a high temperature.

Table 4 (entries 9 to 12) shows the results of glycerol conversion and 1,2-PDO selectivity on Co-MSAPO-11 catalyst as functions of initial H_2 pressure. When changing initial H_2 pressure from 2.0 MPa to 5.0 MPa, it leads to a glycerol conversion and selective formation of 1,2-PDO at about 94.0% and 90.5%, respectively. High pressure allows H_2 easily adsorb on Co metal surface, which facilitates the forward hydrogenated process. These results emphasize that H_2 pressure plays a positive role in the selectivity of the hydrogenation product 1,2-PDO. Obviously, after introducing a higher H_2 pressure (5.0 MPa), glycerol conversion and 1,2-PDO selectivity are stable without considerable increase. For an economic point of view, it is the most suitable way to carry out the catalytic test under initial 4.0 MPa H_2 pressure.

5. Circular Tests

The stability and recyclability of catalyst are considered as important evaluation criteria for industrial applications. Therefore, circular tests were carried out over Co-MSAPO-11 catalyst for glycerol conversion under initial H_2 pressure of 4.0 MPa at 220 °C for 8 h. The results are observed in Table 5. Only 7.8% of glycerol conversion is decreased after third cycle and then sharply drops by 15.7% after the fourth cycle. It can be explained that the organic compound might gradually adsorb on the surface of the catalyst and cause the loss of catalytic activity. However, after the used Co-MSAPO-11 is calcined at 600 °C for 4 h, its catalytic activity is improved with a glycerol conversion of 87.6% (Entry 5). Therefore, it is necessary to use an effective regeneration method for partially deactivated catalyst.

Table 5. The results of the reused Co-MSAPO-11 catalyst[a]

Entry	Conversion [%]	Selectivity [%]
1	90.9	87.6
2	89.2	85.8
3	83.1	84.3
4	75.2	80.2
5	87.6	84.4

[a]Reaction conditions: 4 MPa H_2 pressure, reaction temperature 220 °C and reaction time 8 h.

CONCLUSIONS

A highly active Co-MSAPO-11 catalyst was successfully prepared and used for hydrogenolysis of glycerol to 1,2-PDO. The XRD test showed that the crystal structure of the catalyst sample remains intact after water treatment and high temperature calcination. The results of N_2-physical adsorption, Py-IR and ICP show that the Co-MSAPO-11 catalyst has larger mesoporous size, more L acid sites and actual Co content. In the hydrogenolysis of glycerol, the suitable acidity of Co-MSAPO-11 with more L acidic sites is beneficial to the dehydration of glycerol to produce intermediates acetol. The characteristic micro-mesoporous structure of MSAPO-11 reduces the diffusion barrier of the reactants or products and also provides more effective space for the highly dispersion of Co. Thus, intermediate acetol can be quickly hydrogenated to generate 1,2-PDO in Co metal sites. An appropriate amount of Co (5 wt%) can provide highly dispersed metal active sites without clogging the channel of the catalyst. In summary, the catalytic activity of the Co-MSAPO-11 catalyst is higher than that of the Co-SAPO-11 catalyst and the supported Co/MSAPO-11 catalyst. Under mild conditions (5.0 MPa H_2, 220 °C, and 8 h), 94.0% glycerol conversion and 90.5% selectivity to 1,2-PDO are observed. After repeated cycles of reaction, the surface of the catalyst may accumulate organic compounds to cause a decrease in activity, but the process of high-temperature calcination can regenerate the partially deactivated catalyst. Therefore, this paper brings some important achievements to the conversion of glycerol to commercial product 1,2-PDO.

ACKNOWLEDGEMENT

This work was supported by the National Natural Science Foundation of China under Grant Nos. 21878048 and 21676055.

REFERENCES

1. A. Talebian-Kiakalaieh, N. A. S. Amin and Z. Y. Zakaria, *J. Ind. Eng. Chem.*, **34**, 300 (2016).
2. C. Wei, C. Dasari and M. A. Suppes, *AIChE J.*, **52**, 3543 (2006).
3. M. Pagliaro, R. Ciriminna, H. Kimura, M. Rossi and C. D. Pina, *Angew. Chem. Int. Ed.*, **46**, 4434 (2007).
4. K. Y. Wang, M. C. Hawley and S. J. DeAthos, *Ind. Eng. Chem. Res.*, **42**, 2913 (2003).
5. J. B. Salazar, D. D. Falcone, H. N. Pham, A. K. Datye, F. B. Passos and R. J. Davis, *Appl. Catal. A Gen.*, **482**, 137 (2014).
6. Y. Kusunoki, T. Miyazawa, K. Kunimori and K. Tomishige, *Catal. Commun.*, **6**, 645 (2005).
7. J. T. Dam and U. Hanefeld, *ChemSusChem.*, **4**, 1017 (2011).
8. Y. Amada, Y. Shinmi, S. Koso, T. Kubota, Y. Nakagawa and K. Tomishige, *Appl. Catal. B Environ.*, **205**, 117 (2011).
9. Z. W. Huang, F. Cui, H. X. Kang, J. Chen, X. Z. Zhang and C. G. Xia, *Chem. Mater.*, **20**, 5090 (2008).
10. E. V. Ryneveld, A. S. Mahomed, P. S. van Heerden, M. J. Green and H. B. Friedrich, *Green. Chem.*, **13**, 1819 (2011).

11. E. S. Vasiliadou, E. Heracleous, I. A. Vasalos and A. A. Lemonidou, *Appl. Catal. B Environ.*, **92**, 90 (2009).
12. H. Z. Liu, S. G. Liang, T. Jiang, B. X. Han and Y. X. Zhou, *Clean Soil. Air. Water.*, **40**, 318 (2012).
13. L. Ma and D. He, *Top. Catal.*, **52**, 834 (2009).
14. M. Harisekhar, V. P. Kumar, S. S. Priya and K. V. R. Chary, *J. Chem. Technol. Biotechnol.*, **90**, 1906 (2015).
15. I. Jiménez-Morales, F. Vila, R. Mariscal and A. Jiménez-López, *Appl. Catal. B Environ.*, **117**, 253 (2012).
16. D. Li, Z. W. Zhou, J. Qin, Y. Li, Z. R. Liu and W. L. Wu, *ChemistrySelect.*, **3**, 2479 (2018).
17. R. Rodrigues, N. Isoda, M. Gonçalves, F. C. A. Figueiredo, D. Mandelli and W. A. Carvalho, *Chem. Eng. J.*, **198**, 457 (2012).
18. J. P. Lourenço, A. Fernandes, R. A. Bertolo and M. F. Ribeiro, *RSC Adv.*, **5**, 10667 (2015).
19. Y. Fan, H. Xiao, G. Shi, H. Y. Liu and X. J. Bao, *J. Catal.*, **285**, 251 (2012).
20. Q. Y. Wu, I. N. Oduro, Y. Huang and Y. M. Fang, *Micropor. Mesopor. Mater.*, **218**, 24 (2015).
21. Y. Liu, W. Qu, W. W. Chang, S. X. Pan, Z. J. Tian, X. G. Meng, M. Rigutto, A. van der Made, L. Zhao, X. M. Zheng and F. S. Xiao, *J. Colloid Interface Sci.*, **418**, 193 (2014).
22. X. Li, M. Xiang and D. F. Wu, *Catal. Commun.*, **119**, 170 (2019).
23. S. S. Priya, V. P. Kumar, M. L. Kantam, S. K. Bhargava and K. V. R. Chary, *Catal. Lett.*, **144**, 2129 (2014).
24. R. Arundhathi, T. Mizugaki, T. Mitsudome, K. Jitsukawa and K. Kaneda, *ChemSusChem.*, **6**, 1345 (2013).
25. E. G. Suarez, M. P. Cadenas, A. G. Ruiz, I. R. Ramos and A. Arcoya, *Appl. Surf. Sci.*, **287**, 108 (2013).
26. X. Y. Li, K. W. Li, X. M. Xiang, S. G. Wang, X. C. She, Y. L. Zhu and Y. W. Li, *J. Ind. Eng. Chem.*, **18**, 818 (2012).
27. S. Wang, K. Yin, Y. Zhang and H. Liu, *ACS Catal.*, **3**, 2112 (2013).
28. T. Rajkhowa, G. B. Marin and J. W. Thybaut, *J. Ind. Eng. Chem.*, **54**, 270 (2017).
29. Y. Du, C. C. Wang, H. Jiang, C. L. Chen and R. Z. Chen, *J. Ind. Eng. Chem.*, **35**, 262 (2016).
30. V. Rekha, N. Raju, C. Sumana and N. Lingaiah, *Catal. Lett.*, **147**, 1441 (2017).
31. A. Perosa and P. Tundo, *Ind. Eng. Chem. Res.*, **44**, 8535 (2005).
32. S. Raksaphort, S. Pengpanich and M. Hunsom, *Kinet. Catal.*, **55**, 434 (2014).
33. X. Guo, Y. Li, R. Shi, Q. Liu, E. Zhan and W. Shen, *Appl. Catal. A Gen.*, **371**, 108 (2009).
34. J. W. Bae, S. H. Kang, Y. J. Lee and K. W. Jun, *J. Ind. Eng. Chem.*, **15**, 566 (2009).
35. X. X. Wang, F. Guo, X. X. Wei, Z. M. Liu, W. Zhang, S. Q. Guo and L. F. Zhao, *Korean J. Chem. Eng.*, **33**, 2034 (2016).
36. A. Villa, M. Manzoli, F. Vindigni, L. E. Chinchilla, G. A. Botton and L. Prati, *Catal. Lett.*, **147**, 2523 (2017).
37. L. Guo, Y. Fan, X. J. Bao, G. Shi and H. Y. Liu, *J. Catal.*, **301**, 162 (2013).
38. F. C. Sena, B. F. de Souza, N. C. de Almeida, J. S. Cardoso and L. D. Fernandes, *Appl. Catal. A Gen.*, **406**, 59 (2011).
39. Y. X. Liu, X. M. Liu, L. M. Zhao, Y. C. Lyu, L. Xu, M. J. Rood, L. Wei, Z. Liu and Z. F. Yan, *J. Catal.*, **347**, 170 (2017).
40. T. Jiang, Y. X. Zhou, S. G. Liang, H. Z. Liu and B. X. Han, *Green. Chem.*, **11**, 1000 (2009).